

Sytske Kamminga Kimball*

University of South Alabama, Mobile, Alabama

1. INTRODUCTION

When a hurricane makes landfall, most damage occurs between the time the 17 ms^{-1} isotach touches the coastline and the time the hurricane center crosses the coast. During this time the hurricane moves from shallow coastal waters to solid land, causing an increase in surface roughness and decrease in surface latent heat fluxes which supply the hurricane's energy. These rapidly changing conditions affect the inner-core structure, and hence the distribution, extent, and intensity of damaging winds and rainfall. The underlying physical processes are complex, occur over a very short time (less than a day), and depend on a myriad of complicating factors such as topography, shape of the coastline, angle of incidence of the storm, speed of motion of the storm, and many more. In order to isolate the effects from just the reduction in surface evaporation and the increase in surface roughness, an idealized modeling study is conducted using a west-east oriented, straight coastline with a land surface of 0.1 m elevation, covered by a constant land-use category in both space and time. Simulations making use of different land-use categories, with different roughness length and moisture content properties, are compared. Since the rainfall characteristics have been investigated in detail in a prior study (Kimball, 2008), this paper focuses on the low-level wind structure.

2. MODEL CONFIGURATION

The Penn State/NCAR mesoscale model (MM5) is initialized with a southerly geostrophic wind of 8 m s^{-1} . Embedded in this flow is a hurricane vortex with initial minimum surface pressure (PSMIN) of 970.6 mb and 42 km radius of maximum winds (RMW). The intensity and size properties of this vortex are based on the averaged properties of hurricanes making landfall in the north-central Gulf of Mexico during 1988 - 2002. Construction of such a vortex follows the technique outlined in Kimball and Evans (2002). A 34-hour simulation is conducted using a coarse mesh of 9 km horizontal resolution, a nested grid of 3 km horizontal resolution, and 38 vertical levels. The sea surface temperatures (SSTs) in the model are kept constant at 28°C . Convection is parameterized on the coarse mesh using the Kain-Fritsch scheme and is explicit on the fine mesh. Other parameterizations on both meshes include the Goddard Micro-physics (including graupel) scheme, the MRF boundary layer scheme, a 5-layer

soil model, and a cloud-radiation scheme.

3. EXPERIMENTS

Each simulation differs in the type of land-surface coverage. Four different surfaces with different roughness length (RL) and moisture availability (MA) properties (see Table 1) were chosen. The control simulation (noland) consists of a water surface only.

CASE	ROUGHNESS LENGTH (cm)	MOISTURE AVAILABILITY (%)
savanna	15	15
irrigated	15	50
evergreen	50	50
noland	0	100

Table 1. The moisture availability and roughness length properties of the four experiments.

4. RESULTS

The storms are initially located 200 km south of the straight coastline and move at around 6 m s^{-1} in a northeasterly direction as a result of the environmental steering flow in combination with the β -effect. As the steering flow evolves, the storms gradually slow down until they reach a $3\text{-}4 \text{ ms}^{-1}$ forward speed at $t=20\text{h}$. At $t=15\text{h}$ into the simulation, the storm center crosses the coastline about 220 km east of its original location. At $t=21\text{h}$, the storm tracks curve to follow a more south-southeasterly direction in response to the evolving steering flow.

Figure 1 shows the evolution of storms' maximum windspeed at 10 m height. The noland case shows wind maxima of 36 m s^{-1} or more throughout the entire simulation. The maximum wind is located to the right side of the track, as expected. The landfalling cases display a slightly larger wind maximum than noland (38 m s^{-1} or more) prior to landfall. However, over land the maximum windspeeds drop off drastically, especially in high RL case evergreen. Dry case savanna displays only marginally weaker maximum winds than irrigated (equal RL, but higher MA). These differences can clearly be seen in Figure 2 which displays a timeseries of the maximum winds recorded anywhere in the

* Corresponding author address: Sytske K. Kimball
Univ. of S. Alabama, Dept. Of Earth Sciences, Mobile,
Al, 36688 email:skimball@usouthal.edu

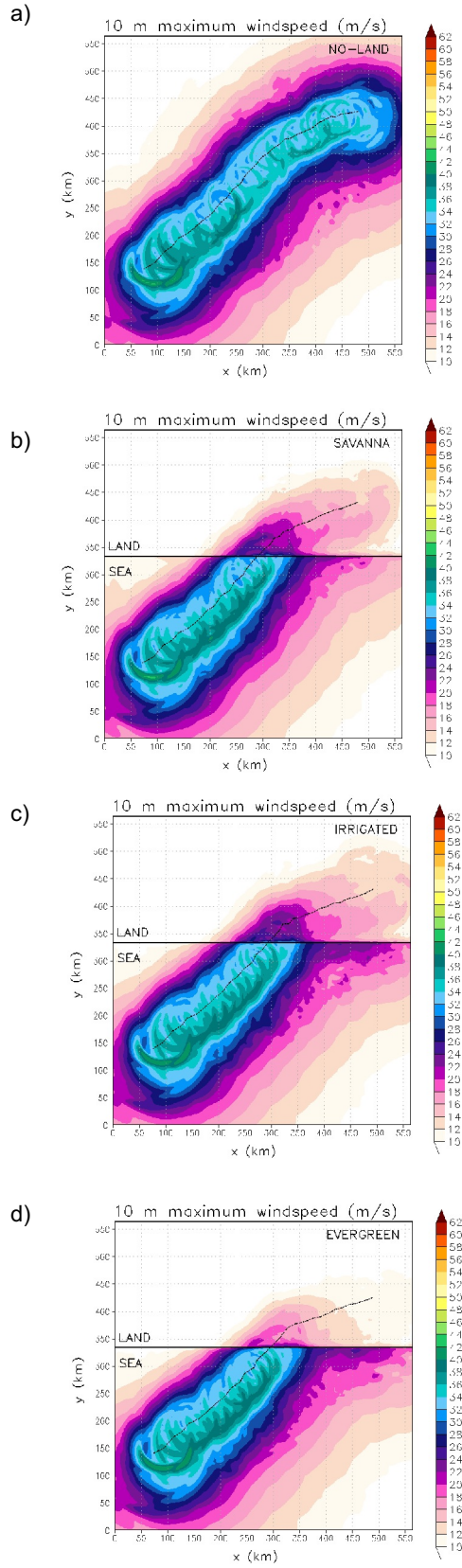


Figure 1: Maximum windspeed (m s^{-1}) recorded at each model grid point during the entire 33h simulation for a) noland, b) savanna, c) irrigated, and d) evergreen.

domain (solid lines) and over land (dashed lines) for all 4 cases at 10m height. The absolute maximum wind remains over water in each case, explaining the differences between the solid and dashed curves. At 45 and 125 m, the absolute maximum wind remains located over land and high RL case evergreen still displays weaker winds over land than the other cases but the difference reduces from about 8 to 5 m s^{-1} . By 230 m height, there no longer is a difference between the dashed and solid curves, hence, the maximum wind is found over land in all cases. However the values for evergreen remain about 4 m s^{-1} lower than the other landfalling cases. Evergreen displays lower maximum winds than the other cases at all levels investigated (3 km and below).

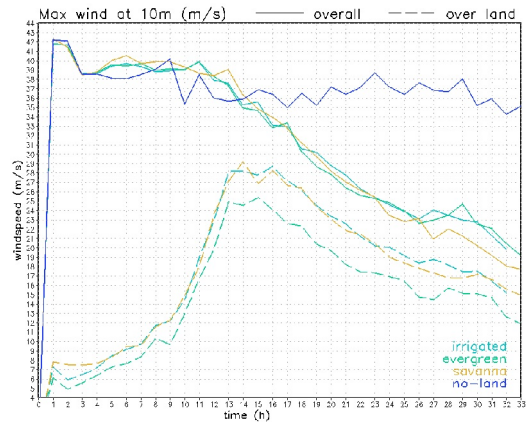


Figure 2: Timeseries of the 10 m maximum windspeed anywhere in the domain (solid curves) and over land (dashed curves) for all 4 cases.

The same evolution is seen in the minimum surface pressure (not shown) with irrigated being the strongest storm, savanna about 0.5 hPa weaker than irrigated, and evergreen about 3 hPa weaker than savanna.

In this section, the maximum wind at each of 24 azimuths is explored. Figure 3 shows the spread of the maximum wind at 10 m for each time step for noland, irrigated, and evergreen. Case no-land displays much less scatter in maximum windspeed values than the landfalling cases. After landfall, evergreen displays more scatter than no-land, as expected. In all 3 cases, the absolute maximum wind is located in the south-east quadrant. With a north-eastward moving storm this coincides with 'to the right of the storm track'.

Figure 4 shows that the azimuthal location of the absolute maximum at 10 m height varies considerably in the noland case. Especially during its phase of intensification (Figure 3a). This was when the storm became more symmetric, moved more slowly and no

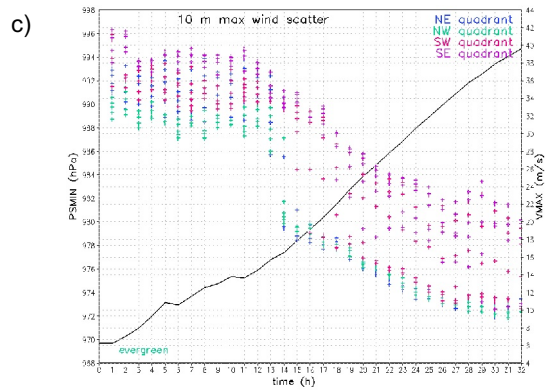
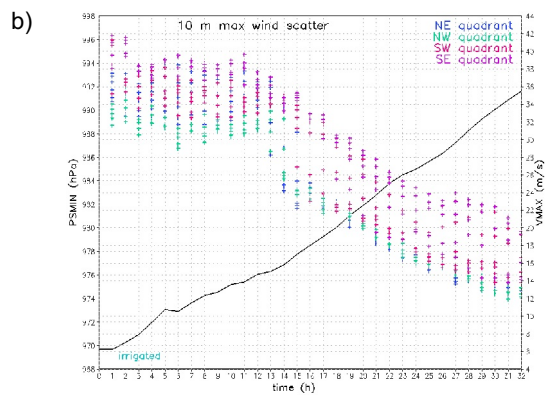
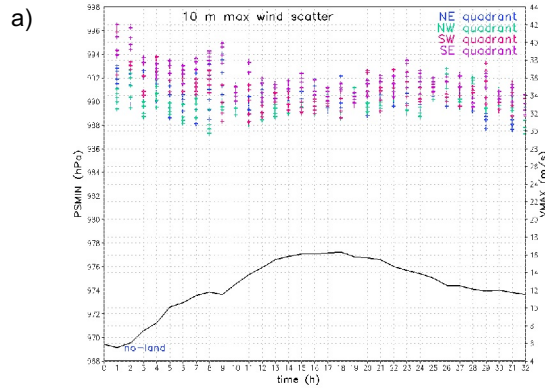


Figure 3: Timeseries of maximum 10 m wind (m s^{-1}) at each of 24 azimuths (colored crosses) and minimum surface pressure (hPa, solid black line) for a) no-land, b) irrigated, and c) evergreen.

preferred location for the maximum wind existed. In the landfalling cases, the 10 m maximum wind resides in the south-east quadrant and moves to the south of the storm center after landfall ($t=15\text{h}$) where stronger, on-shore winds are located.

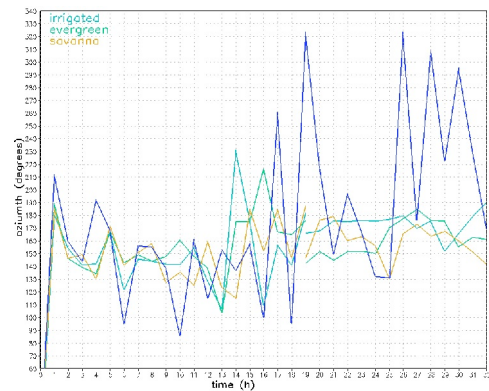


Figure 4: Azimuth of the location of the 10 m maximum wind over water (before $t=19\text{h}$) and over land (after $t=19\text{h}$).

5. DISCUSSION

The roughness length seems to play a larger role than the moisture availability in weakening a landfalling storm in terms of maximum windspeed as well as minimum surface pressure. Storm motion plays a dominant role in determining the azimuthal location of the maximum windspeed at levels below 3 km, although previous work indicated that dry air intrusion plays a large role (Kimball, 2008). For these north-eastward moving storms, the maximum wind is located in the south-east quadrant or to the right of the storm track. Once the storms cross the coastline, the maximum wind at the lowest levels (below about 150 m) remains over water. This explains the large spread with azimuth of 10 m maximum wind values for the same minimum surface pressure in the landfalling cases. The maximum windspeed over land can be found to the south of the storm center where the winds come off the water. The azimuthal spread of 10 m maximum winds is enhanced for cases with higher surface roughness. These large spreads in maximum wind values make estimations of the maximum wind for a given minimum surface pressure a challenging task.

Acknowledgments

This work is supported by NSF Award No. ATM-0239492 and by NOAA Award No. NA06NWS4680008. This work was made possible in part by a grant of high performance computing resources and technical support from the Alabama Supercomputer Authority.

6. REFERENCES

- Kimball S.K. and J. L. Evans, 2002: Idealized numerical modeling of hurricane-trough interaction. *Mon. Wea. Rev.*, **130**, 2210-2227.
- Kimball, S. K., 2008: Structure and evolution of rainfall in numerically simulated landfalling hurricanes. *Mon. Wea. Rev.*, In Press.